

UC San Diego

UC San Diego Previously Published Works

Title

Coherent structure of zonal flow and onset of turbulent transport

Permalink

<https://escholarship.org/uc/item/2tw370vv>

Journal

Physics of Plasmas, 12(6)

ISSN

1070-664X

Authors

Itoh, K
Hallatschek, K
Itoh, S-I
[et al.](#)

Publication Date

2005-06-01

DOI

10.1063/1.1922788

Copyright Information

This work is made available under the terms of a Creative Commons Attribution-NonCommercial-NoDerivatives License, available at <https://creativecommons.org/licenses/by-nc-nd/4.0/>

Peer reviewed

Coherent structure of zonal flow and onset of turbulent transport

K. Itoh

National Institute for Fusion Science, Toki 509-5292, Japan

K. Hallatschek

Max-Planck-Institut für Plasmaphysik, 85748 Garching, Germany

S.-I. Itoh

Research Institute for Applied Mechanics, Kyushu University, Kasuga 816-8580, Japan

P. H. Diamond

Department of Physics, University of California–San Diego, San Diego, California 92093-0319

S. Toda

National Institute for Fusion Science, Toki 509-5292, Japan

(Received 16 January 2005; accepted 4 April 2005; published online 26 May 2005)

Excitation of the turbulence in the range of drift wave frequency and zonal flow in magnetized plasmas is analyzed. Nonlinear stabilization effect on zonal flow drive is introduced, and the steady state solution is obtained. The condition for the onset of turbulent transport is obtained and partition ratio of fluctuation energy into turbulence and zonal flows is derived. The turbulent transport coefficient, which includes the effect of zonal flow, is also obtained. Analytic result and direct numerical simulation show a good agreement. © 2005 American Institute of Physics.

[DOI: 10.1063/1.1922788]

I. INTRODUCTION

Turbulent transport in high temperature plasmas is one of the main issues in modern plasma physics. Microscopic fluctuations are induced owing to the gradients of plasma pressure and magnetic field so as to enhance the cross-field transport of energy far beyond the level that is determined by the binary collision of charged particles. In the development of theory and direct nonlinear simulation (DNS) of turbulent transport in toroidal plasmas, it has been clarified that the plasma turbulence in the range of drift wave frequency, which we abbreviate “drift waves” in this article, plays key roles.^{1,2} What is fascinating is that the zonal flow,³ which is constant on magnetic surface but changes rapidly across magnetic surfaces, is induced by turbulent fluctuations and, at the same time, suppresses the turbulent transport. The generation of zonal flow has been confirmed by DNS (see, e.g., Refs. 4 and 5 and the review in Ref. 6 for a full description). Zonal flow in the core plasma has been observed in experiment very recently.⁷ The problem of zonal flow generation by pressure gradient has a wide and deep impact on the plasma physics. The zonal flow is associated with the vorticity which is almost constant on magnetic field. That is, a global axial vector field is generated. The problems of the generation of global axial vector field from the gradient of scalar field include the geodynamo solar magnetic field generation or astronomical jet formation.^{8,9} The turbulence and zonal flow in toroidal plasmas provide an opportunity to investigate this class of problems with theory, DNS, and experimental observation, simultaneously. Intensive studies of the system of zonal flow and drift wave turbulence have been performed. The achievements so far have been summarized in the review in Ref. 6.

One of the key issues is the mechanism that regulates the

structure of the induced zonal flows. The saturation mechanisms of zonal flow have been discussed in the literature; while the turbulence is often completely quenched for weakly unstable cases at the collisionless limit,^{10–13} stationary states with finite amplitudes of both the zonal flow and turbulent fluctuations are realized when the plasmas are in highly unstable states. The possibility of secondary instabilities has been pointed out,^{14–18} and the condensation of micromodes into global modes has been studied by direct nonlinear simulations (DNS).¹⁹ Regarding the theoretical formulation of nonlinear processes, nonlinearity in the self-interaction of zonal flows has also been investigated. Research has included the pursuit of the possibility that the zonal flows evolve into a kink-soliton-like structure,²⁰ the parametric evolution of a plane drift wave,²¹ and the theory for the BGK (Bernstein–Greene–Kruskal) solution has also been developed.^{22–24} The importance of random noise to turbulence has been studied (e.g., Refs. 25 and 26), and influences of turbulent noise on zonal flow has also been studied.^{3,24,27} Drift wave spectrum was analyzed in the presence of zonal flow,²⁸ and dynamical evolution has also been studied.²⁹ Although these models provide useful understanding, they are not free from limitations. For instance, the accessibility to the kink-soliton-like solution from a small initial perturbation in Ref. 20 is not clear; the drift waves often develop into strong turbulence so that the assumption that the plane drift wave will be coherent may be violated, and the decorrelation time of the drift wave packet is often shorter than the circumnavigation time of the packet in the zonal flow trough. Theoretical efforts are still required for the study of zonal flow structure in cases where drift waves have short correlation times. In addition, it is known that the tor-

oidal geometry is crucial in determining the structure of turbulence and flow.^{13,30–33}

In this article, we analyze the nonlinear state of zonal flow which is driven by fluctuations in the drift-wave-frequency range in toroidal plasmas, in the case that the autocorrelation times of drift waves are much shorter than that of the zonal flow. (The study of such a case is motivated by the DNS of core plasmas for highly unstable cases. It is clearly shown in Ref. 34 that the half width at half maximum of the spectral intensity of the zonal flow is much narrower than that of turbulence.) It was shown, for given fluctuation amplitude in toroidal plasmas, that $\Pi_{\theta r}$ (the transport of perpendicular momentum in the radial direction) shows a nonlinear saturation with respect to the zonal flow shear, while $\Pi_{\parallel r}$ (the transport of parallel momentum in the radial direction) does not.³² That is, the drive of the zonal flow starts to decrease at high velocity, but the damping due to the turbulent viscosity of parallel flow does not. Therefore, the zonal flow evolves into a nonlinear stationary state, and the stable coherent structure is obtained. In this article, the higher-order corrections by zonal flow on the zonal flow drive is renormalized, and the driving term at an arbitrary magnitude of zonal flow vorticity is derived. Based on the nonlinear form of the zonal flow growth rate, the steady state solution is obtained. In the collisionless limit, the turbulence level is shown to vanish while the zonal flow remains at finite amplitude, when instability is weak. The critical condition for the onset of drift wave turbulence in the presence of zonal flow is derived. This gives a theoretical explanation for the Dimits shift phenomena. The turbulent transport, including the zonal flow effects, is obtained. The partition ratio of fluctuating field energy among the drift wave turbulence and zonal flow is also obtained. A comparison with DNS is also made.

II. THE MODEL

A. Formulation based on drift wave action

We study the system of the drift-wave (DW) turbulence and zonal flow (ZF) in inhomogeneous and magnetized plasma. The model dynamical system for the drift wave action N_k and the zonal flow velocity V_Z has been studied.²⁰ The drift wave action N_k has been introduced as

$$N_k = (1 + k_{\perp}^2 \rho_s^2) |\tilde{\phi}_k|^2, \quad (1)$$

where $\tilde{\phi}_k$ is the k -Fourier component of electrostatic perturbation of drift waves, k_{\perp} is the wavenumber of drift waves perpendicular to the main magnetic field and ρ_s is the ion gyroradius at electron temperature. In this article, the analysis is developed following the framework which utilizes the coupled equations for N_k and V_Z . (For the survey of methods of analysis for zonal flows, see Ref. 6.)

The growth of the zonal flow in the presence of the drift-wave turbulence has been discussed by use of the time scale separation. The autocorrelation times of the drift wave fluctuations are assumed to be much faster than the evolution time of the zonal flow. In the slow time scale, the evolution of the zonal flow and the drift wave action is governed by²⁰

$$\frac{\partial}{\partial t} U = \frac{\partial^2}{\partial r^2} \frac{c^2}{B^2} \int d^2k \frac{k_{\theta} k_r}{(1 + k_{\perp}^2 \rho_s^2)^2} \hat{N}_k - \gamma_{\text{damp}} U, \quad (2)$$

and by the eikonal equation

$$\frac{\partial}{\partial t} N_k + \frac{\partial \omega_k}{\partial \mathbf{k}} \cdot \frac{\partial N_k}{\partial \mathbf{x}} - \frac{\partial \omega_k}{\partial \mathbf{x}} \cdot \frac{\partial N_k}{\partial \mathbf{k}} = 0, \quad (3)$$

where U is the vorticity of the zonal flow

$$U = \partial V_Z / \partial r, \quad (4)$$

r is the minor radius, \hat{N}_k is a slow modulation of N_k , which is induced by V_Z , and γ_{damp} denotes the damping rate of zonal flow by other processes.

We study the case that the zonal flow retains the coherent structure in a time much longer than the decorrelation time of the drift wave fluctuations. This ‘‘coherent regime’’ is one of the characteristic situations of the DW-ZF system,⁶ and is observed in various simulation conditions.¹³ Equation (3) is solved by expansion with respect to the vorticity of the zonal flow as

$$\hat{N}_k = \hat{N}_k^{(1)} + \hat{N}_k^{(2)} + \hat{N}_k^{(3)} \cdots, \quad (5)$$

where $\hat{N}_k^{(j)}$ is the j th order term of U . (An explicit form of expansion parameter is explained later.) Substitution of Eq. (5) into Eq. (2) provides

$$\frac{\partial}{\partial t} U = \sum_m^{\infty} G^{(m)} - \gamma_{\text{damp}} U, \quad (6a)$$

where the m th order term with respect to U in the Reynolds stress is expressed as

$$G^{(m)} = \frac{\partial^2}{\partial r^2} \frac{c^2}{B^2} \int d^2k \frac{k_{\theta} k_r}{(1 + k_{\perp}^2 \rho_s^2)^2} \hat{N}_k^{(m)}. \quad (6b)$$

A linear response has been obtained from Eq. (3) as²⁰

$$\hat{N}_k^{(1)} = k_{\theta} U R(q_r, \Omega) \frac{\partial N_k}{\partial k_r}. \quad (7)$$

Here

$$R(q_r, \Omega) = \frac{i}{\Omega - q_r v_{\text{gr}} + i \Delta \omega_k} \quad (8)$$

is the response function, $\Delta \omega_k$ is the nonlinear broadening of drift waves,

$$v_{\text{gr}} = \partial \omega / \partial k_r \quad (9)$$

is the group velocity, and the zonal flow has a slow dependence as

$$\exp(iq_r r - i\Omega t) \quad (10)$$

(q_r is the radial modenummer of zonal flow).

The higher order responses with respect to U , $\hat{N}_k^{(2)}$, $\hat{N}_k^{(3)}$, ..., can be calculated from

$$\hat{N}_k^{(n)}(q_r + q_r') = U R(q_r + q_r', \Omega) k_\theta \frac{\partial}{\partial k_r} \hat{N}_k^{(n-1)}(q_r'), \quad (11)$$

where $\hat{N}_k^{(n-1)}(q_r')$ represents the q_r' -Fourier component. The group velocity v_{gr} is an antisymmetric function of k_r for drift waves in this article. Therefore, $R(q_r, \Omega)$ has a symmetry with respect to k_r . The contributions from the even order terms $\hat{N}_k^{(2m)}$ ($m=1, 2, 3, \dots$) are small from the consideration of symmetry, and the drive of ZF comes from the odd order terms $\hat{N}_k^{(2m+1)}$ ($m=0, 1, 2, \dots$). In addition, when q_r is chosen in the regime where the zonal flow has maximum growth rate, the higher-harmonics components with nq_r ($n=3, 4, \dots$) have large damping rates.^{6,35} Therefore we keep $2q_r$ -component and have a relation

$$\hat{N}_k^{(n)} = U^2 k_\theta^2 R^*(q_r, \Omega) \frac{\partial}{\partial k_r} \left(R(2q_r, \Omega') \frac{\partial \hat{N}_k^{(n-2)}}{\partial k_r} \right), \quad (12)$$

where $\hat{N}_k^{(n)}$ is the abbreviation of $\hat{N}_k^{(n)}(q_r)$.

B. Linear response

The first-order term gives the diffusion-like form

$$\gamma_Z = D_{rr} q_r^2 = -D_{rr} \partial^2 / \partial r^2 \quad (13)$$

in Eq. (2) with

$$D_{rr} = -\frac{c^2}{B^2} \int d^2k \frac{R(q_r, \Omega) k_\theta^2 k_r}{(1 + k_\perp^2 \rho_s^2)^2} \frac{\partial N_k}{\partial k_r}, \quad (14)$$

i.e., the zonal flow growth.³ In a case that the decorrelation rate of zonal flow is large, $\Delta\omega_k \gg q_r v_{gr}$,

$$R(q_r, \Omega) \simeq 1/\Delta\omega_k. \quad (15)$$

The partial integral of Eq. (14) gives an evaluation

$$D_{rr} = \frac{c^2}{B^2} \int d^2k \frac{k_\theta^2}{(1 + k_\perp^2 \rho_s^2)^2 \Delta\omega_k} N_k. \quad (16)$$

Next, the most unstable wavenumber of the zonal flow is considered. The zonal flow growth rate γ_Z does not continue to increase at larger q_r when the dispersion effect of the beat drift waves on the zonal flow is introduced. A finite- q_r correction to $R(q_r, \Omega)$ is evaluated in the large $\Delta\omega_k$ limit by expanding $R(q_r, \Omega)$ to

$$R(q_r, \Omega) = \frac{1}{\Delta\omega_k} \left(1 - \left(\frac{q_r v_{gr}}{\Delta\omega_k} \right)^2 + \dots \right), \quad (17)$$

and γ_Z is written as

$$\gamma_Z = D_{rr} q_r^2 (1 - q_r^2 / K_0^2), \quad (18)$$

where

$$K_0^2 = \Delta\omega_k^2 (v_{gr})^{-2} \quad (19)$$

represents the characteristic scale where the Doppler-shift of drift waves suppresses the zonal flow instability. An explicit form of K_0^2 for the case of tokamak plasmas is given in Ref. 21. It should also be noted that expression (2) is drawn with the condition that $q_r < k_r$. The analysis in the case of $q_r \sim k_r$ was reported based on a modulational instability, showing

that the zonal mode drive vanishes if $q_r > k_r$.³⁵ We have

$$K_0 = \min(k_r, \Delta\omega_k / v_{gr}). \quad (20)$$

The damping term $\gamma_{damp} U$ includes the collisional damping term $\nu_{damp} U$. An additional damping mechanism exists. The $E \times B$ flow in toroidal plasma is associated with the secondary flow. As is shown in Refs. 30–32, the viscous damping of the secondary flow due to toroidicity governs the damping rate of the zonal flow, in addition to the conventional collisional damping. The damping rate by this process is rewritten as³¹

$$\gamma_{damp} = \mu_{||} (1 + 2q^2) q_r^2, \quad (21)$$

where $\mu_{||}$ is the turbulent shear viscosity for the flow along the field line and q is the safety factor. (The coefficient $1 + 2q^2$ is replaced by $1 + 1.6q^2 / \sqrt{\epsilon}$ in the collisionless limit.³⁶ This dependence on the collisionality is not considered for simplicity.) Combining this damping associated with parallel flow, the damping rate is expressed as

$$\gamma_{damp} = \nu_{damp} + \mu_{||} (1 + 2q^2) K^2. \quad (22)$$

And an explicit form of ν_{damp} is given in, e.g., Ref. 6,

$$\nu_{damp} \simeq \frac{\nu_{ii}}{\epsilon} \quad (23)$$

in the banana regime.

Combining these results, the linear terms in Eq. (2) are rewritten as

$$\begin{aligned} \frac{\partial}{\partial t} U + D_{rr} \left(\frac{\partial^2}{\partial r^2} U + K_0^{-2} \frac{\partial^4}{\partial r^4} U \right) - \mu_{||} (1 + 2q^2) \frac{\partial^2}{\partial r^2} U \\ + \nu_{damp} U = 0. \end{aligned} \quad (24)$$

This equation predicts a necessary condition for the zonal flow growth with the wavenumber q_r at which the linear growth rate of zonal flow takes the maximum value. The zonal flow has a maximum growth rate at

$$q_r = q_r^* = \sqrt{\frac{1 - \mu}{2}} K_0, \quad (25)$$

where

$$\mu \equiv \mu_{||} (1 + 2q^2) D_{rr}^{-1}. \quad (26)$$

The condition that the zonal flow has positive linear growth rate is given as

$$1 - \mu > 2 \sqrt{\frac{\nu_{damp}}{D_{rr} K_0^2}}. \quad (27)$$

Both the zonal-flow driving coefficient D_{rr} and the shear viscosity $\mu_{||}$ are given by drift wave spectrum N_k . The ratio $\mu \equiv \mu_{||} (1 + 2q^2) D_{rr}^{-1}$ is a function of the spectral shape of drift wave turbulence and geometrical factor such as q , the inverse aspect ratio ϵ , etc.

C. Third-order correction

The third-order term of the deformed action is given as

$$\hat{N}_k^{(3)} = U^2 k_\theta^2 R^*(q_r, \Omega) \frac{\partial}{\partial k_r} \left(R(2q_r, \Omega) \frac{\partial \hat{N}_k^{(1)}}{\partial k_r} \right). \quad (28)$$

Substituting Eq. (28) into Eq. (6b), one obtains the third-order term on the right-hand side (RHS) of Eq. (2) as

$$G^{(3)} = \frac{\partial^2 c^2}{\partial r^2 B^2} \int U^2 d^2 k \frac{k_\theta^3 k_r}{(1 + k_\perp^2 \rho_s^2)^2} R^*(q_r, \Omega) \frac{\partial}{\partial k_r} \left(R(2q_r, \Omega') \frac{\partial \hat{N}_k^{(1)}}{\partial k_r} \right). \quad (29)$$

In a strong turbulence limit, $\Delta\omega_k \gg q_r v_{gr}$, which gives an estimate Eq. (16) through partial integral, the RHS of Eq. (29) is evaluated as

$$G^{(3)} = - \frac{\partial^2 c^2}{\partial r^2 B^2} \int U^2 d^2 k \frac{k_\theta^3}{(1 + k_\perp^2 \rho_s^2)^2} R^*(q_r, \Omega) R(2q_r, \Omega') \times \frac{\partial \hat{N}_k^{(1)}}{\partial k_r}. \quad (30)$$

The partial integral is performed once again. Noting the relation

$$\frac{\partial}{\partial k_r} \left(\frac{R^*(q_r, \Omega) R(2q_r, \Omega')}{(1 + k_\perp^2 \rho_s^2)^2} \right) \simeq - \frac{H}{\Delta\omega_k^2} \frac{k_r \rho_s^2}{(1 + k_\perp^2 \rho_s^2)^2} \quad (31a)$$

with a coefficient

$$H = \frac{2}{1 + k_\perp^2 \rho_s^2} + \frac{6q_r^2}{\Delta\omega^2 \rho_s^2} \frac{\partial v_g}{\partial k_r^2}, \quad (31b)$$

[where the second term on the RHS of Eq. (31b) is a finite wavenumber correction], we have an estimate of the third-order term as

$$G^{(3)} = - \frac{\partial^2 c^2}{\partial r^2 B^2} \int d^2 k \left(\frac{H k_\theta^2 \rho_s^2 U^2}{\Delta\omega_k^2} \right) \frac{k_\theta k_r}{(1 + k_\perp^2 \rho_s^2)^2} \hat{N}_k^{(1)} = \frac{\partial^2}{\partial r^2} D_3 U^3, \quad (32)$$

where the diffusion coefficient in the third-order term is given as

$$D_3 = - \frac{c^2}{B^2} \int d^2 k \left(\frac{H k_\theta^2 \rho_s^2}{\Delta\omega_k^2} \right) \frac{k_\theta k_r}{(1 + k_\perp^2 \rho_s^2)^2} \hat{N}_k^{(1)}. \quad (33)$$

Comparing Eq. (33) with Eq. (16), we finally have an estimate of the diffusion coefficient of the third-order term as

$$D_3 \simeq \frac{H k_\theta^2 \rho_s^2}{\Delta\omega_k^2} D_{rr}. \quad (34)$$

The sign in the definition of D_3 is chosen such that D_3 is positive when D_{rr} is positive.

Taking into account Eqs. (24) and (32), Eq. (2) is written in an explicit form as

$$\frac{\partial}{\partial t} U + D_{rr} \left(\frac{\partial^2}{\partial r^2} U + K_0^{-2} \frac{\partial^4}{\partial r^4} U \right) - D_3 \frac{\partial^2}{\partial r^2} U^3 - \mu_\parallel (1 + 2q^2) \frac{\partial^2}{\partial r^2} U + \nu_{\text{damp}} U = 0 \quad (35)$$

up to the third order with respect to U . The expansion parameter is $H k_\theta^2 \rho_s^2 U^2 / \Delta\omega_k^2$ in deriving Eq. (35).

D. Renormalization of higher order corrections

Equation (35) allows one to study the radial structure of the nonlinear solution. The truncation at the third order may not be appropriate if

$$H k_\theta^2 \rho_s^2 U^2 > \Delta\omega_k^2 \quad (36)$$

holds. Therefore, the third-order formula is not relevant for the study of the Dimits shift, where the fluctuation level is very low so that $\Delta\omega_k^2$ is small. In order to study the case of an arbitrary ratio of $H k_\theta^2 \rho_s^2 U^2 / \Delta\omega_k^2$, we must keep all order of U . In this section, we discuss the renormalization of the driving term $\sum_{m=0}^{\infty} G^{(2m+1)}$. By the renormalization method, the summation provides a screened form of the Reynolds stress which is extended to the parameters like Eq. (36). (See, e.g., Ref. 38 for details.)

The radial wavelength of the zonal flow is taken as $2\pi/q_r^*$, and is treated as a parameter in this section. By employing this simplification, we derive a recurrence formula between $G^{(2m+1)}$ and $G^{(2m-1)}$ in the following. The $(2m+1)$ th order term of Eq. (6b) is written as

$$G^{(2m+1)} = - q_r^2 \frac{c^2}{B^2} \int d^2 k \frac{k_\theta k_r}{(1 + k_\perp^2 \rho_s^2)^2} \hat{N}_k^{(2m+1)} \quad (37)$$

and is rewritten as

$$G^{(2m+1)} = - q_r^2 \frac{c^2}{B^2} \int d^2 k \frac{k_\theta^3 k_r}{(1 + k_\perp^2 \rho_s^2)^2} U^2 R^*(q_r, \Omega) \frac{\partial}{\partial k_r} \left(R(2q_r, \Omega') \frac{\partial \hat{N}_k^{(2m-1)}}{\partial k_r} \right). \quad (38)$$

In the case of the strong turbulence, Eq. (15), a similar argument to Eq. (16) is employed for Eq. (38). Thus, performing a partial integration twice, one has

$$G^{(2m+1)} = q_r^2 \frac{c^2}{B^2} \int d^2 k \left(\frac{H k_\theta^2 \rho_s^2 U^2}{\Delta\omega_k^2} \right) \frac{k_\theta k_r}{(1 + k_\perp^2 \rho_s^2)^2} \hat{N}_k^{(2m-1)}. \quad (39)$$

That is, one obtains a relation between $G^{(2m+1)}$ and $G^{(2m-1)}$ as

$$G^{(2m+1)} \simeq - \frac{H k_\theta^2 \rho_s^2 U^2}{\Delta\omega_k^2} G^{(2m-1)}. \quad (40)$$

The result Eq. (40) indicates that the ratio $|G^{(2m+1)} / G^{(2m-1)}|$ diverges as $\Delta\omega_k \rightarrow 0$ for a fixed value of U . However, such singular behavior does not occur. This is because the decorrelation between the drift wave packet and the zonal flow is not given by $\Delta\omega_k$ but by other processes, when $\Delta\omega_k$ approaches zero. Therefore we put

$$G^{(2m+1)} \simeq -\frac{Hk_{\theta}^2 \rho_s^2 U^2}{\Gamma^2} G^{(2m-1)} \quad \text{as } \Delta\omega_k \rightarrow 0, \quad (41)$$

where Γ is the decorrelation rate between zonal flow and waves in the small $\Delta\omega_k$ limit. One decorrelation process is the Doppler shift, and $q_r v_{gr}$ plays a role that limits the resonance between zonal flow and drift waves. The other relevant frequency is the bounce frequency ω_b of the drift wave packet in the trough of the zonal flow,²²

$$\omega_b^2 = \frac{2\rho_s^2 k_{\theta} q_r}{1 + \rho_s^2 k_{\theta}^2} \omega_k U. \quad (42)$$

That is, Γ scales with $\max(\omega_b, q_r v_{gr})$. The quantitative determination of the proportionality constant between Γ and $\max(\omega_b, q_r v_{gr})$ requires the detailed analysis of the turbulent trapping regime, such as the granulation formalism.³⁷ Thus we choose here

$$\Gamma = \max(\omega_b, q_r v_{gr}). \quad (43)$$

It should be noticed that Eq. (40) does not mean $G^{(2m+1)}$ remains finite as $\Delta\omega_k \rightarrow 0$. It means that the ratio $|G^{(2m+1)}/G^{(2m-1)}|$ remains finite. In the limit where $\Delta\omega_k = 0$ holds and the trapping of wavepacket occurs, the net driving force of the zonal flow can vanish and the solution can be given by BGK (Bernstein–Greene–Kruskal) solution. Within the framework of the model of this article, Eq. (14) indicates that $G^{(1)}$ vanishes (so does $G^{(2m+1)}$) as $\Delta\omega_k \rightarrow 0$. Thus this model provides renormalization in the case of finite $\Delta\omega_k$ and partly recovers the property in the limit of wave trapping. Taking a Padé approximation, one has an interpolation formula as

$$G^{(2m+1)} \simeq -\frac{Hk_{\theta}^2 \rho_s^2 U^2}{\Delta\omega_k^2 + \Gamma^2} G^{(2m-1)}. \quad (44)$$

That is,

$$G^{(2m+1)} \simeq (-1)^m \left(\frac{U^2}{\Delta\omega_k^2 + \Gamma^2} \frac{Hk_{\theta}^2 \rho_s^2}{Hk_{\theta}^2 \rho_s^2} \right)^m G^{(1)}. \quad (45)$$

By use of the formula (44), the summation $\sum_{m=0}^{\infty} G^{(2m+1)}$ can be calculated. We have the renormalized driving term for the zonal flow as

$$\sum_{m=0}^{\infty} G^{(2m+1)} = \frac{G^{(1)}}{1 + \frac{Hk_{\theta}^2 \rho_s^2 U^2}{\Delta\omega_k^2 + \Gamma^2}}. \quad (46)$$

In Eq. (46), the nonlinear correction up to all orders are included. The evolution equation for the zonal flow Eq. (6a) is then written as

$$\frac{\partial}{\partial t} U = \frac{q_r^2 D_{rr}}{1 + \frac{Hk_{\theta}^2 \rho_s^2 U^2}{\Delta\omega_k^2 + \Gamma^2}} U - (\mu_{\parallel}(1 + 2q^2)q_r^2 + \nu_{\text{damp}})U. \quad (47)$$

III. NONLINEAR RADIAL EIGENMODE IN COLLISIONLESS LIMIT

In this section, we study the nonlinear eigenmode of zonal flow for given drift wave fluctuations by keeping the third-order nonlinear term. We take a limit of

$$\nu_{\text{damp}} \rightarrow 0, \quad (48)$$

because the role of the nonlinear stabilization term in Eq. (35) is studied. We use normalized variables

$$x = r/L, \quad \tau = t/t_Z, \quad u = U/U_0, \quad (49)$$

where

$$L^{-2} = K_0^2(1 - \mu), \quad t_Z = D_{rr}^{-1} K_0^{-2}(1 - \mu)^{-2}, \quad (50)$$

$$U_0^2 = D_{rr} D_3^{-1}(1 - \mu).$$

Equation (35) is rewritten as ($\nu_{\text{damp}} \rightarrow 0$)

$$\frac{\partial}{\partial \tau} u + \frac{\partial^2}{\partial x^2} u - \frac{\partial^2}{\partial x^2} u^3 + \frac{\partial^4}{\partial x^4} u = 0. \quad (51)$$

The short wavelength components with $q_r^2 L^2 > 1$ are stabilized by the higher-order derivative term. The flow is generated in the long wavelength region of

$$q_r^2 < K_0^2(1 - \mu), \quad (52)$$

and the zonal flow energy is saturated by the nonlinearity and by the dissipation through higher-order derivatives.

We investigate a case that the flow is generated from the state with small noise level where no net flow exists,

$$\int dx u = 0. \quad (53)$$

Conservation of total momentum holds for the periodic boundary condition and the flow evolves satisfying the condition $\int dx u = 0$. Stationary solution of Eq. (51) in the domain $0 < x < d$, for the periodic boundary condition, is given by an elliptic integral as

$$\int (1 - 2u^2 + u^4 - \kappa^2)^{-1/2} du = \pm \frac{x}{\sqrt{2}}, \quad (54)$$

where κ is an integral constants satisfying $0 \leq \kappa < 1$ and is determined from the periodicity

$$\int_{-u_c}^{u_c} (1 - 2u^2 + u^4 - \kappa^2)^{-1/2} du = \frac{d}{2\sqrt{2n}}, \quad (55a)$$

where

$$u_c = \sqrt{1 - \kappa}, \quad (55b)$$

and $n = 1, 2, 3, \dots$

The temporal evolution of Eq. (51) is solved numerically. Starting from an initial condition with small random values, a stable steady state is reached. It is shown that the growth is dominated by the component which has the largest linear growth rate. That is, the integer n is given by the one which is closest to

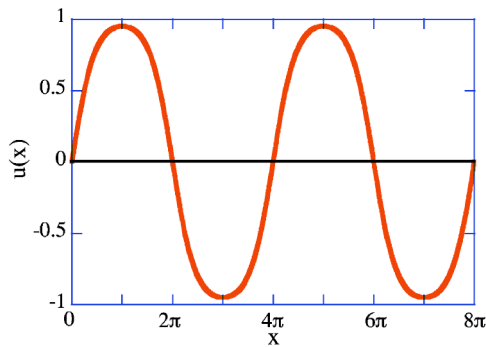


FIG. 1. Stationary state of the normalized solution $u(x)$ for the case of $d = 8\pi$. Radial length x and vorticity u are normalized values.

$$d/n = 4\sqrt{2}\pi. \quad (56)$$

Figure 1 illustrates the stable stationary state. The peak value of $u(x)$ is given as $u_c \approx 0.95$. Compared to a simple sinusoidal function (eigenfunction of linear operator), the result in Fig. 1 has much weaker curvature at the peak and is closer to a piecewise constant function. The result Eq. (56) shows that the characteristic wavelength of the zonal flow is controlled by K_0 , the parameter dependence of which is expressed in Eq. (20).

The stationary state is realized by the balance between the drive of zonal flow through $d\Pi_{\theta r}/dr$ and the damping through $d\Pi_{\parallel r}/dr$. (Π is the Reynolds stress.) The $d\Pi_{\theta r}/dr$ term is composed of the second and third terms on the left-hand side (LHS) of Eq. (35) (having coefficients D_{rr} and D_3). The $d\Pi_{\parallel r}/dr$ term corresponds to the fourth term on the LHS of Eq. (35), having coefficients μ_{\parallel} . When the zonal flow amplitude is small and Eq. (27) holds, the drive by $d\Pi_{\theta r}/dr$ exceeds the damping by $d\Pi_{\parallel r}/dr$ so that the zonal flow grows. When the ZF amplitude increases, the nonlinear term in $d\Pi_{\parallel r}/dr$ becomes effective, and $d\Pi_{\theta r}/dr$ starts to decrease. At the amplitude of zonal flow where $d\Pi_{\theta r}/dr + d\Pi_{\parallel r}/dr = 0$ holds, the zonal flow reaches the stationary state.

IV. SELF-CONSISTENT STATE

Based on the analysis of the stationary coherent structure of zonal flow, we study the self-consistent state for the DW-ZF system. The condition for the excitation of drift waves in the presence of zonal flow and the energy partition of between the drift wave and zonal flow is discussed. Then the transport coefficient by drift wave turbulence, where the effect of zonal flow is included, is derived.

A. Model of coupled equations

1. Low-degree-of-freedom model

The self-consistent state of zonal flow and drift wave has been studied theoretically by solving the evolution of the spectrum of drift waves.²⁸ The studies have shown that a low-degree-of-freedom model, such as predator-pray model, is useful in giving a qualitative understanding of the self-consistent state. In addition, the study of the nonlinear radial

wave form in Sec. III gives us the result that the structure is well represented by a few parameters like amplitude and periodicity length.

Based on the results in Sec. III, we choose the periodic length $2\pi q_r^{-1}$ of the zonal flow as

$$q_r \rho_i \approx \frac{\sqrt{1-\mu}}{2} K_0 \rho_i, \quad (57)$$

and employ the dynamical equation in which q_r is treated as a parameter. Under this circumstance, the equation for the amplitude of the zonal flow is then given as Eq. (47). By use of this simplification, both the collisionless case and the weakly collisional case are studied here.

The back interaction of the zonal flow on drift wave turbulence has been discussed in detail. In order to show the argument with analytic transparency, we choose a simplest model for the evolution of drift wave amplitude after Refs. 3 and 39 as

$$\frac{\partial}{\partial t} \hat{\phi}^2 = \gamma_L \hat{\phi}^2 - \alpha \hat{\phi}^2 \hat{W} - \Delta\omega \hat{\phi}^2, \quad (58)$$

where γ_L is the growth rate of the turbulence energy and $\hat{\phi}$ is the normalized fluctuation amplitude

$$\hat{\phi}^2 = \left(\frac{k_{\perp}^2 L_n}{k_{\theta}} \right)^2 \left| \frac{e\tilde{\phi}}{T} \right|^2, \quad (59)$$

and $|\tilde{\phi}|$ is an amplitude of drift wave fluctuations, γ_L is the linear growth rate, the nonlinear damping rate $\Delta\omega$ shows the effect of the nonlinear interactions within drift wave turbulence, the rate α that satisfies

$$2D_{rr} q_r^2 = \alpha \hat{\phi}^2 \quad (60)$$

is used according to the convention of Ref. 3, and

$$\hat{W} = (U/\omega_*)^2 \quad (61)$$

is the normalized square amplitude of the zonal flow vorticity.

With a similar procedure, Eq. (47) is rewritten as

$$\frac{\partial}{\partial t} \hat{W} = \frac{\alpha \hat{\phi}^2}{1 + \frac{Hk_{\theta}^2 \rho_s^2 \omega_*^2}{\Delta\omega_k^2 + \Gamma^2} \hat{W}} \hat{W} - (\mu\alpha \hat{\phi}^2 + 2\nu_{\text{damp}}) \hat{W}, \quad (62)$$

where $\mu_{\parallel}(1+2q^2)q_r^2$ term is rewritten as $\mu\alpha\hat{\phi}^2$ by use of Eqs. (26) and (60).

Equations (58) and (62) form a set of coupled dynamical equations for the DW-ZF system in a reduced model.

2. Evaluation of the nonlinear damping term

We here estimate $\Delta\omega_k$ in various cases. In the strong turbulence limit of drift wave fluctuations, $\Delta\omega_k$ is estimated as¹

$$\Delta\omega_k \approx B^{-1} k_{\perp}^2 |\tilde{\phi}|. \quad (63)$$

It is rewritten as

$$\Delta\omega_k \approx \omega_* \hat{\phi} \quad (64)$$

by use of the normalized drift wave amplitude. In a weak turbulence limit, one has

$$\Delta\omega_k \approx \omega_* \hat{\phi}^2. \quad (65)$$

3. Coupled dynamical equations

The relation between the fluctuation level and nonlinear decorrelation rate, Eq. (64) or Eq. (65), closes the set of equations. The nonlinear damping rate by drift wave turbulence is chosen here as Eq. (64) for the strong turbulence. This choice is motivated by the fact that an explicit formula is obtained in the presence of collisional damping and renormalized nonlinear damping for zonal flows. (Of course, the strong turbulence limit may not be valid near the Dimits shift boundary in the absence of collisional damping of zonal flow. The limit of $\nu_{\text{damp}} \rightarrow 0$ is explained in Sec. IV B 3.) By this simple model, Eqs. (58) and (62) take form as

$$\frac{\partial}{\partial t} \hat{\phi}^2 = \gamma_L \hat{\phi}^2 - \alpha \hat{\phi}^2 \hat{W} - \omega_* \hat{\phi}^3, \quad (66)$$

and

$$\frac{\partial}{\partial t} \hat{W} = \frac{\alpha \hat{\phi}^2}{1 + \frac{Hk_{\theta}^2 \rho_s^2 \omega_*^2}{\omega_*^2 \hat{\phi}^2 + \Gamma^2}} \hat{W} - (\mu \alpha \hat{\phi}^2 + 2\nu_{\text{damp}}) \hat{W}, \quad (67)$$

respectively. The set of equations (66) and (67) describes the partition of fluctuation energy into drift waves and zonal flows.

B. Solution and energy partition

1. Domain of solutions

Equation (67) gives the condition for the stationary state for the zonal flow. Putting $\partial/\partial t=0$ in Eq. (67), one has

$$\frac{Hk_{\theta}^2 \rho_s^2 \omega_*^2}{\omega_*^2 \hat{\phi}^2 + \Gamma^2} \hat{W} = \frac{\alpha \hat{\phi}^2}{\mu \alpha \hat{\phi}^2 + 2\nu_{\text{damp}}} - 1, \quad (68)$$

or

$$\hat{W} = 0. \quad (69)$$

From Eq. (68), one sees that the nontrivial solution $\hat{W} \neq 0$ is allowed for

$$\hat{\phi}^2 = \hat{\phi}_{\text{th}}^2, \quad (70)$$

where

$$\hat{\phi}_{\text{th}}^2 = \frac{2\nu_{\text{damp}}\alpha^{-1} - g + \mu w + \sqrt{(2\nu_{\text{damp}}\alpha^{-1} - g + \mu w)^2 + 8(g + (1 - \mu)w)\nu_{\text{damp}}\alpha^{-1}}}{2(1 - \mu)}, \quad (71)$$

and abbreviations are

$$g = (1 - \mu)\Gamma^2\omega_*^{-2}, \quad w = Hk_{\theta}^2 \rho_s^2 \omega_*^2 \hat{W}. \quad (72)$$

The zonal flow grows as $\hat{\phi}^2 > \hat{\phi}_{\text{th}}^2$, and damps for $\hat{\phi}^2 < \hat{\phi}_{\text{th}}^2$. Figure 2 illustrates $\hat{\phi}_{\text{th}}^2$ as a function of the zonal flow vorticity for various values of collisional damping.

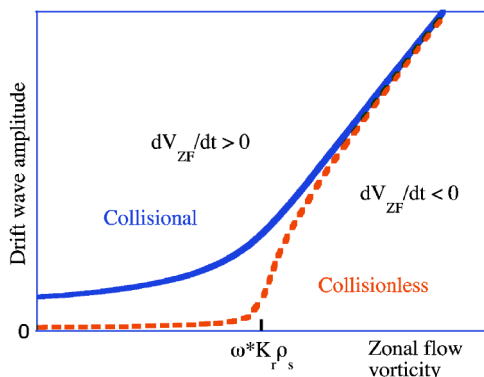


FIG. 2. The diagram for the zonal flow growth on $(\hat{U}, \hat{\phi})$ plane. Solid line indicates the neutral condition for the weakly collisional case, and the dashed line is for the collisionless case.

Equation (71) provides various limiting results. In a limit of small zonal flow vorticity, $\hat{W} \rightarrow 0$, Eq. (71) takes a form

$$\hat{\phi}_{\text{th}}^2 = \frac{2\nu_{\text{damp}}}{(1 - \mu)\alpha}, \quad (73)$$

which shows that the fluctuation level is regulated by the damping rate of the zonal flow. This recovers the previous result, although a screening factor by the return flow is included in Eq. (73).

The other limit of interest is the collisionless limit, $\nu_{\text{damp}}/\alpha \rightarrow 0$. In this case, the stationary state of Eq. (62) provides

$$\frac{\Delta\omega_k^2}{\omega_*^2} = \frac{\mu Hk_{\theta}^2 \rho_s^2}{(1 - \mu)} \hat{W} - \frac{\Gamma^2}{\omega_*^2}. \quad (74)$$

This result has two specific features. First, $\Delta\omega_k$ vanishes (i.e., $\hat{\phi}$ vanishes) at a critical vorticity of zonal flow,

$$U = U_c, \quad (75a)$$

where

$$U_c^2 = \frac{(1 - \mu)}{\mu Hk_{\theta}^2 \rho_s^2} \Gamma^2, \quad (75b)$$

i.e.,

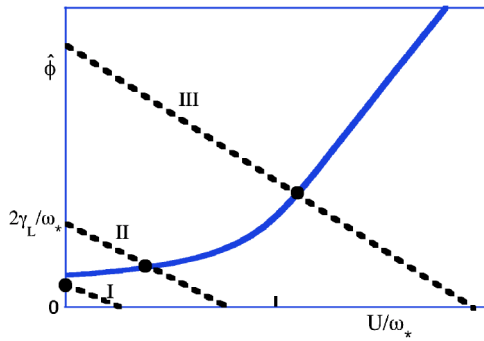


FIG. 3. Three cases for the solutions. Solid line indicates the marginal condition for the zonal flow growth. Dotted lines denote those for the drift waves for various values of linear growth rate. Dots indicate steady-state solutions. If the drive of drift wave is weak [case I], the steady state solution is given by zero zonal flow. The intermediate case [II] and strong drive case [III] are also shown.

$$U_c = \max\left(\frac{2(1-\mu)}{\mu H}, \sqrt{\frac{2(1-\mu)}{\mu H}} k_r \rho_s\right) q_r V_d, \quad (75c)$$

where use was made of Eqs. (42) and (43). (V_d is the diamagnetic velocity.) On the RHS of Eq. (75c), the first term in parentheses is given when Γ is evaluated by ω_b and the second one is given when Γ is evaluated by $q_r v_{gr}$. Equation (75a) means that the growth of zonal flow remains marginal at this critical vorticity even in the limit of small drift wave fluctuation level. This nonlinear balance at the limit of weak drift wave fluctuations is related to the Dimits shift problem, and is discussed in later sections. Note that Eqs. (74) and (75a)–(75c) hold without depending on the assumption of strong or weak turbulence limit.

Next, Eq. (74) provides a law of power partition between zonal flow and drift waves. In a limit of strong fluctuations and flow, $U \gg U_c$, Eq. (74) gives a relation

$$\frac{\Delta \omega_k^2}{\omega_*^2} = \frac{\mu H k_\theta^2 \rho_s^2}{(1-\mu)} \hat{W}. \quad (76a)$$

This relation is rewritten in the limit of strong turbulence in a dimensional form as

$$U = \frac{k_\perp^2 c_s}{\sqrt{\mu H} k_\theta} \frac{e \tilde{\phi}}{T}. \quad (76b)$$

2. Stationary solutions

We next consider the balance between the drift wave amplitude and that of the zonal flow. The stationary state of drift wave turbulence is given from Eq. (66)

$$\hat{\phi} = \frac{\gamma_L}{\omega_*} - \frac{\alpha}{\omega_*} \hat{W}, \quad (77)$$

or

$$\hat{\phi}^2 = 0. \quad (78)$$

Combining Eq. (71) with Eq. (77), the self-consistent solution is obtained. Figure 3 illustrates the self-consistent

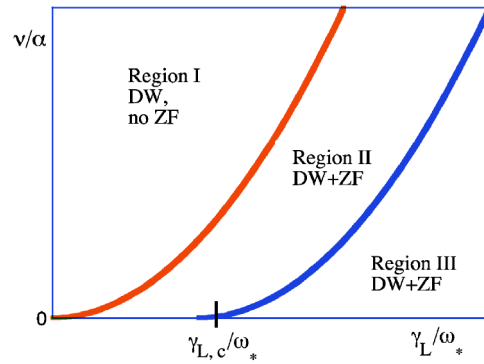


FIG. 4. Domains in control parameters. (In this diagram, the time rate α is treated as a constant parameter.)

solution schematically. Owing to the kink of the boundary of Eq. (71) at $U \approx U_c$, there arise three regions.

In the region of small growth rate of drift waves,

$$\frac{\gamma_L}{\omega_*} < \sqrt{\frac{2\nu_{\text{damp}}}{(1-\mu)\alpha}} \quad (\text{region I}) \quad (79)$$

there is no crossing of lines (71) and (77). Therefore, only the solution Eq. (69) is allowed, and one has the solution

$$\hat{\phi} = \frac{\gamma_L}{\omega_*} \quad (\text{region I}) \quad (80a)$$

with

$$\hat{W} = 0. \quad (80b)$$

The zonal flow is not excited, and the turbulence level is not influenced by the zonal flow.

In an intermediate region,

$$\sqrt{\frac{2\nu_{\text{damp}}}{(1-\mu)\alpha}} < \frac{\gamma_L}{\omega_*} < \sqrt{\frac{2\nu_{\text{damp}}}{(1-\mu)\alpha}} + \frac{\alpha}{\omega_*} U_c^2 \quad (\text{region II}), \quad (81)$$

the boundary for the stationary zonal flow is given by Eq. (73). The collisional damping controls the steady state solution. In region II, analytic forms of fluctuation level and zonal flow amplitude are

$$\hat{\phi} = \sqrt{\frac{2\nu_{\text{damp}}}{(1-\mu)\alpha}} \quad (\text{region II}) \quad (82a)$$

and

$$\hat{W} = \frac{\gamma_L}{\alpha} - \frac{\omega_*}{\alpha} \sqrt{\frac{2\nu_{\text{damp}}}{(1-\mu)\alpha}}, \quad (82b)$$

respectively. In this region, the zonal flow amplitude increases as γ_L increases, but the turbulence level is unchanged. The fluctuation level $\hat{\phi}^2$ is proportional to the collisional damping rate of the zonal flow. This reproduces the preceding result of theory and DNS observations.^{10,21,29}

When the growth rate becomes larger,

$$\frac{\gamma_L}{\omega_*} > \sqrt{\frac{2\nu_{\text{damp}}}{(1-\mu)\alpha}} + \frac{\alpha}{\omega_*} U_c^2 \quad (\text{region III}). \quad (83)$$

Equations (76a) and (76b) describes the balance of the zonal flow. The self-nonlinear damping of the zonal flow dominates the steady state. In a strongly unstable limit,

$$\frac{\gamma_L}{\omega_*} \gg \sqrt{\frac{2\nu_{\text{damp}}}{(1-\mu)\alpha}}, \quad U \gg U_c \quad (84)$$

one has

$$\hat{\phi} = \sqrt{\frac{\gamma_L \mu H k_{\theta}^2 \rho_s^2}{\alpha (1-\mu)}} \quad (\text{region III}) \quad (85a)$$

and

$$\hat{W} = \frac{\gamma_L}{\alpha}. \quad (85b)$$

When the growth rate becomes larger, the zonal flow velocity and the fluctuation level increase as γ_L increases.

Figure 4 summarizes the characteristic domains in the parameter space. Figure 5 illustrates the wave amplitude $\hat{\phi}$ or $\Delta\omega_k/\omega_*$ and the zonal flow vorticity U/ω_* as a function of the growth rate. Figure 5(a) illustrates the case in the presence of the collisional damping of the zonal flow. Three regions appear.

3. Collisionless limit and upshift of excitation boundary

Here, the problem of the upshift of the critical condition in terms of the linear growth rate is discussed. [Here, the assumption of the strong turbulence limit, Eq. (64) is not employed.] In the collisionless limit,

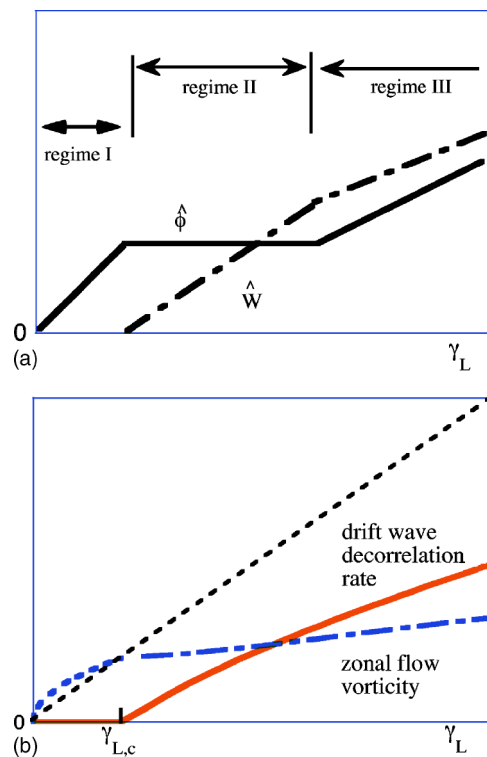


FIG. 5. The dependence of the amplitude of drift wave fluctuations $\hat{\phi}$ (solid line) zonal flow \hat{W} (chained line) vs γ_L in the collisional case (a). (Here, ν/ω_* and α/ω_* are kept constant.) Three regions appear. The decorrelation rate of drift wave $\Delta\omega_k/\omega_*$ (solid line) and zonal flow vorticity \hat{W} (thick broken line and thick dashed line) in the collisionless case $\nu=0$ are given in (b). Thin dotted line shows $\Delta\omega_k/\omega_*$ when zonal flows are not taken into account. (α/ω_* is kept constant.) The drift wave amplitude $\hat{\phi}$ is related to $\Delta\omega_k/\omega_*$ as is shown in Eq. (64) or (65). Region I disappears, and the drift waves are excited in region III.

$$\nu_{\text{damp}} \rightarrow 0, \quad (86)$$

Eqs. (58) and (62) provide a steady-state solution as

$$\frac{\Delta\omega_k}{\omega_*} = \frac{-\frac{\mu H k_{\theta}^2 \rho_s^2 \omega_*}{(1-\mu)\alpha} + \sqrt{\left(\frac{\mu H k_{\theta}^2 \rho_s^2 \omega_*}{(1-\mu)\alpha}\right)^2 + 4\left(\frac{\mu H k_{\theta}^2 \rho_s^2 \gamma_L}{(1-\mu)\alpha} - \frac{\Gamma^2}{\omega_*^2}\right)}}{2}, \quad (87)$$

if the growth rate exceeds a critical value

$$\gamma_L > \gamma_{L,c} \equiv \frac{(1-\mu)\alpha \Gamma^2}{\mu H k_{\theta}^2 \rho_s^2 \omega_*^2}. \quad (88)$$

Below this critical growth rate, $\gamma_L < \gamma_{L,c}$, we have

$$\hat{\phi} = 0. \quad (89)$$

In the vicinity of the critical condition, $\gamma_L \sim \gamma_{L,c}$, Eq. (87) provides

$$\frac{\Delta\omega_k}{\omega_*} = \frac{1}{\omega_*} (\gamma_L - \gamma_{L,c}). \quad (90)$$

The fluctuation amplitude is calculated from the formula of $\Delta\omega_k$, Eq. (87), by use of Eq. (64) or (65), depending on whether it is in the weak turbulence regime or in the strong turbulence regime.

From Eq. (90), one sees that the drift wave fluctuations are, in the limit of vanishing collisional damping of the zonal flow, sustained at finite levels when the growth rate of modes γ_L exceeds a finite threshold value $\gamma_{L,c}$. This is a theoretical explanation for the Dimits shift, which has been observed in

numerical simulations. Note that, in the limit of large growth rate, $\gamma_L \gg \gamma_{L,c}$, Eq. (85a) is reproduced from Eq. (87). Figure 5(b) shows the collisionless limit. In this case, region I disappears, and transition between regions II and III is seen.

4. Partition of energy between DW and ZF

Combining Eqs. (71) and (77), the amplitudes of the zonal flow and drift waves are determined simultaneously. Thus the partition of energy between the zonal flow and wave turbulence is given. The partition of energy is evaluated by the ratio $V_{ZF}^2/\tilde{V}_{DW}^2$ where V_{ZF} is the velocity of zonal flow, $k_\theta q_r^{-1} V_d \sqrt{\hat{W}}$, and \tilde{V}_{DW} is the fluctuating $E \times B$ velocity of drift wave fluctuations, $k_\theta k_\perp^{-1} V_d \hat{\phi}$. This ratio is given as

$$\frac{V_{ZF}^2}{\tilde{V}_{DW}^2} = \frac{k_\perp^2 \hat{W}}{q_r^2 \hat{\phi}^2} = \frac{4}{1 - \mu K_0^2} \frac{k_\perp^2 \hat{W}}{\hat{\phi}^2}. \quad (91)$$

In the strong turbulence limit in region III, one has a relation from Eqs. (76a) and (76b), and the energy partition is given as

$$\frac{V_{ZF}^2}{\tilde{V}_{DW}^2} = \frac{4}{\mu H k_\theta^2 \rho_s^2 K_0^2} \frac{k_\perp^2}{\hat{\phi}^2}. \quad (92)$$

The flow energy and wave energy are proportional to each other. In the strong turbulence limit, the energy can be converted into flow energy more than to the wave fluctuation energy if $k_\theta^2 \rho_s^2 < 4/\mu H$ holds.

C. Turbulent transport coefficient

The analysis in Sec. IV B gives an insight into the turbulence and turbulent transport. The ion thermal conductivity is deduced for the drift wave turbulence which is dressed by zonal flows. The ion thermal conductivity is evaluated as¹

$$\chi_i = \Delta \omega_k k_r^{-2}. \quad (93)$$

By use of the dependence of $\Delta \omega_k$ on the amplitude of drift wave fluctuations, Eq. (64), χ_i is evaluated, for the strong turbulence limit, as

$$\chi_i = \frac{k_\theta}{k_r^2 \rho_i} \left(\frac{v_{thi} \rho_i^2}{L_n} \right) \hat{\phi}. \quad (94)$$

The quantity $(k_\theta/k_r^2 \rho_i) v_{thi} \rho_i^2 L_n^{-1}$ is the so-called gyro-Bohm diffusion coefficient. Equations (80a), (82a), and (85a) show the fluctuation amplitude as a function of the growth rate in various regions, showing the effects of zonal flow.

The thermal conductivity in the case of the weak growth rate of drift waves and strong damping of zonal flow [region I] is given from Eqs. (80a) and (94) as

$$\chi_i = \frac{\gamma_L}{k_r^2} \quad (\text{region I}). \quad (95)$$

In this case, there is no zonal flow in the steady state, and this agrees with the case of ‘‘bare’’ drift waves. When growth rate of drift wave becomes larger (and yet the collisional damping dictates the zonal flow) [region II], the conductivity is given as

$$\chi_i = \sqrt{\frac{2\nu_{\text{damp}}}{(1-\mu)\alpha}} \frac{\omega_*}{k_r^2} \quad (\text{region II}). \quad (96)$$

In region III, the saturation level of the zonal flow is determined by the nonlinear process of zonal flow, not by the collisional damping. Therefore the formula for the collisionless limit is useful. In the collisionless limit, Eqs. (87) and (93) provide the formula of thermal conductivity as

$$\chi_{\text{III}} = \frac{\mu H k_\theta^2 \rho_s^2 \omega_*}{(1-\mu)\alpha} \left(\frac{-1 + \sqrt{1 + \frac{4(1-\mu)\alpha}{\mu H k_\theta^2 \rho_s^2 \omega_*^2} (\gamma_L - \gamma_{L,c})}}{2} \right) \frac{\omega_*}{k_r^2} \quad (\text{region III}). \quad (97)$$

This form of χ_{III} becomes finite, $\chi_{\text{III}} \geq 0^2$, for $\gamma_L \geq \gamma_{L,c}$. [Note again that Eq. (97) does not depend on the limits (64) or (65).] In this collisionless case, in the vicinity of the nonlinear onset condition $\gamma_L \approx \gamma_{L,c}$, Eq. (97) provides a simplified expression of the transport coefficient as

$$\chi_i = \frac{\gamma_L - \gamma_{L,c}}{k_r^2}. \quad (98)$$

One might be interested in more specific case studies. In the framework that the wavelength is much longer than ρ_s and $k_r \rho_s \ll 1$, in small $\Delta \omega_k$ -limit, the decorrelation between drift wave and zonal flow is determined by the wave-bounce frequency. We have

$$\Gamma^2 = \frac{2\rho_s^2 k_\theta^2 q_r}{(1 + \rho_s^2 k_\theta^2)^2} V_d U, \quad (U > U_c) \quad (99)$$

from Eq. (42), and the critical vorticity is given from Eq. (75c) as

$$U_c = (2(1-\mu)/\mu H) q_r V_d. \quad (100)$$

At this critical vorticity, ω_b and Γ are evaluated as

$$\Gamma = \sqrt{\frac{4(1-\mu)}{\mu H} \frac{\rho_s q_r}{1 + \rho_s^2 k_\theta^2} \omega_*}. \quad (101)$$

Substituting Eq. (101) into Eq. (88), the critical growth rate is evaluated as

$$\gamma_{L,c} = \frac{4(1-\mu)^2 q_r^2}{\mu^2 H^2} \frac{1}{k_\theta^2} \alpha. \quad (102)$$

The boundary for the onset of turbulence has a dependence as $\gamma_{L,c} \propto q_r^2 k_\theta^{-2} \alpha$ with a numerical factor.

For practical usage, it is useful to have an interpolation formula of χ_i in these three regions. In regions I and II, χ_i may be fitted as

$$\chi_i = \chi_{\text{I+II}} \equiv \frac{\gamma_L \sqrt{\frac{2\nu_{\text{damp}}}{(1-\mu)\alpha}} \frac{\omega_*}{k_r^2}}{\gamma_L + \sqrt{\frac{2\nu_{\text{damp}}}{(1-\mu)\alpha}} \omega_*}. \quad (103)$$

This type of interpolation formula has been derived in, e.g., Ref. 40. A possible fitting formula for all three regions is

$$\chi_i = \sqrt{\chi_{I+II}^2 + \chi_{III}^2 \Theta(\gamma_L - \gamma_{L,c})}, \quad (104)$$

where $\Theta(\gamma_L - \gamma_{L,c})$ is a Heaviside function, $\Theta(\gamma_L - \gamma_{L,c})=1$ for $\gamma_L > \gamma_{L,c}$ and $\Theta(\gamma_L - \gamma_{L,c})=0$ for $\gamma_L < \gamma_{L,c}$. This formula covers both the collisional regime (regions I and II) and the self-nonlinearity regime (region III), including the property like Dimits shift.

The thermal conductivity in the presence of zonal flow in regions II and III, Eqs. (96) and (97), is much reduced, in comparison with the case of “bare” drift waves (i.e., ZF neglected), for which Eq. (95) is given. The reduction factor, in regions II and III, \mathbf{R} , can be defined accordingly.⁴¹ An example of transport coefficient in explicit form is discussed in the appendix.

D. Comparison with nonlinear simulation

1. Global parameter dependence

It is worthwhile to compare these theoretical results with DNS. The result is tested to the result of a three-dimensional nonlinear simulation of the ion-temperature-gradient (ITG) mode turbulence based on two fluid models.¹³ In this simulation, the dynamics of the electrostatic potential, ion temperature, and ion parallel velocity are followed in toroidal geometry with an assumption of adiabatic response for electrons. Radial width of simulation domain is $120\rho_i$ and a realistic ITG dynamic was obtained by switching off the unrealistically high parallel fluid heat conduction. Parameters are $\epsilon_n \equiv 2L_n/R=0.9$, $L_n/L_{Ti}=3.1$, $q=1.4$ ($q=0.7$ for zonal flow component in order to reduce the damping of zonal flow), and $s=0.8$. (L_n and L_{Ti} are gradient scale lengths of density and temperature, respectively and s : magnetic shear). Details are explained in Ref. 13.

In the analytic theory, the ITG mode is characterized by the modenumber

$$k_\theta \rho_i \sim \frac{1}{3}, \quad (105a)$$

and

$$k_\theta \sim k_r. \quad (105b)$$

This set of parameters, Eqs. (105a) and (105b), are chosen as an input to this theory, and the level of zonal flow is analytically estimated, and is compared with the result of DNS.

In this section, we derive the relation between U and χ_i by employing Eq. (93), because these values of parameters are reported in DNS results.¹³ It should be noted that this comparison is possible in the collisionless limit, even if one does not assume the strong turbulence limit or weak turbulence limit, Eqs. (64) or (65). (The investigation⁴² has shown that the relation between χ_i and $\hat{\phi}$ is in between the strong turbulence limit (Eq. (64), $\chi_i \propto \hat{\phi}$) and the weak turbulence limit (Eq. (65), $\chi_i \propto \hat{\phi}^2$). Reference 42 reports that the case there is closer to the weak turbulence limit.) In units of $V_d \rho_i^{-1}$, the zonal flow vorticity is given by $U = k_\theta \rho_i \sqrt{W} V_d \rho_i^{-1}$ where V_d is the diamagnetic drift velocity. By use of Eq. (105a), we have

$$U = \frac{1}{3} \sqrt{W} V_d \rho_i^{-1}, \quad (106a)$$

and the relation

$$\chi_i = 3 \frac{\Delta \omega_k}{\omega_*} (v_{thi} \rho_i^2 L_n^{-1}) \quad (106b)$$

is deduced from Eq. (93) by use of Eq. (105b).

For the case when the parallel flow damping has considerable influence in modifying the quasilinear growth rate of the zonal flow (such as the DNS parameter in Ref. 13), we choose a representative value of $\mu \sim 1/2$. For the parameters Eqs. (105a) and (105b), one has $H \sim 2.5$. With the help of the relation for K_0 in Refs. 21, 35 of $K_0 \sim sk_\theta$, one has

$$q_r \approx 0.1 \rho_s^{-1} \quad (107)$$

for the wavenumber of the zonal flow. By use of these parameters, Eq. (100) provides an estimate

$$U_c \sim 0.085 V_d \rho_i^{-1}, \quad (108)$$

at the boundary for the onset of turbulence, and the steady state condition Eq. (74) is written as

$$\frac{\Delta \omega_k}{\omega_*} = \frac{\sqrt{2.5} \rho_s}{V_d} \sqrt{U^2 - U_c U} = \frac{\sqrt{2.5} \rho_s}{V_d} \sqrt{U^2 - 0.085 V_d \rho_s^{-1} U} \quad (109)$$

in the collisionless limit. Combining Eqs. (106b) and (109), the relation between χ_i and U , $\chi_i(U)$, is derived as

$$\frac{\chi_i}{v_{thi} \rho_i^2 L_n^{-1}} = 4.7 \frac{\rho_i}{V_d} \sqrt{U^2 - \frac{0.085 V_d}{\rho_i} U}. \quad (110)$$

It is emphasized again that the estimate of $\mu \sim 1/2$ and Eq. (105a) and (105b) are the input parameters, which are used to derive the theoretical prediction Eq. (110).

Equation (110) is compared with DNS in Fig. 6. Solid line shows the theory [Eq. (110)] and dots denote the result of DNS. A fairly good agreement between them is observed, and theoretical results, e.g., Eq. (110), are not rejected. We should note here that the fact that the cut-off frequency Γ is introduced based on an order-of-magnitude estimate, and the relation of the thermal transport coefficient [e.g., Eq. (93)] has an ambiguity of numerical factor. Thus, one should not expect an exact agreement of the DNS data and the theoretical result Eq. (110), but should focus on the qualitative feature, such that the appearance of the cut-off at small drift wave amplitude or an asymptotic relation $\chi_i \propto U$ in the limit of large turbulent transport. It should be noted that, strictly speaking, Eq. (93) is not tested by Ref. 13. (In the series of simulations in Fig. 6, the larger thermal conductivity is realized for more strongly unstable cases. This suggests the increment of the turbulence decorrelation rate of waves in conjunction with the increment of thermal conductivity.) The final conclusion, whether this theory explains the DNS or not, must be drawn after the test of Eq. (93) is made in DNS under the condition of Fig. 6.

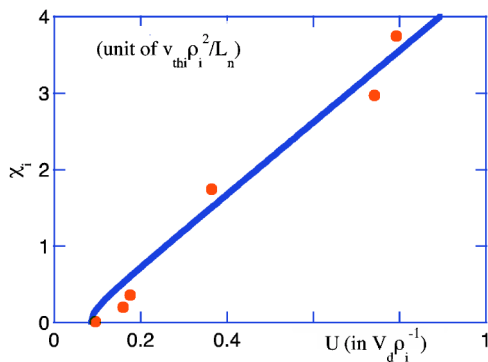


FIG. 6. Comparison of the relations $\chi_i(U)$ for the steady state of ITG mode. Zonal flow vorticity is measured in units of $V_d \rho_i^{-1}$ and thermal conductivity is in $v_{thi} \rho_i^2 L_n^{-1}$. Theory (solid line) and DNS data (dots) are quoted from Ref. 13.

2. Radial profile of nonlinear eigenmode

Before closing the analysis, the radial profile of the induced zonal flow is also compared with the DNS. For the parameters of interest, the model theory provides the radial periodicity length as $\lambda \sim 60 \rho_i$ from Eq. (107). Figure 7 illustrates the radial distribution of the vorticity associated with the zonal flow, $d\langle v_y \rangle / dr$, where $\langle \dots \rangle$ denotes the average over the magnetic surface and r and y coordinates are taken in the radial and poloidal directions, respectively. The simulation result confirms this theoretical modelling. First, the radial distribution of the vorticity shows the flattened quasi-periodic form. This is an extreme case of relatively low dispersion and high linear drive in the analytic result. Second, the periodic length is about

$$\lambda \sim 30 \rho_i \quad (111)$$

and is in the range of theoretical prediction. Third, the magnitude of the vorticity is $d\langle v_y \rangle / dr \sim 0.6 V_d \rho_i^{-1}$. This value is also in the range of theoretical prediction, $U_0 \sim 0.45 V_d \rho_i^{-1}$ at

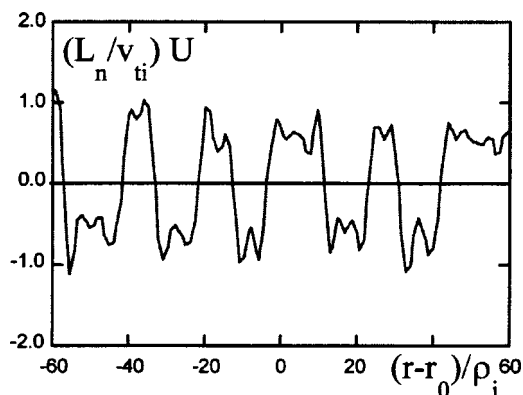


FIG. 7. Radial distribution of vorticity of zonal flow U in the DNS. Snapshot in the stationary state is shown. Origin of radius r_0 is chosen at the center of simulation box.

$\Delta\omega \sim \omega_s$. The agreement of the magnitude of zonal flow between theory and DNS is already explained in Sec. IV D 1.

V. SUMMARY AND DISCUSSION

In summary, we have developed a theory of nonlinear evolution of the drift wave-zonal flow system. In the regime where coherent structure of zonal flow survives much longer than the decorrelation time of drift waves, the coherent structure of the zonal flow was analyzed. The self-nonlinear effect of zonal flow realizes the stationary state. The coherent structure of zonal flow was studied by the perturbative expansion with respect to the zonal flow amplitude. The nonlinear radial eigenmode was expressed in terms of elliptic integral. This determines the characteristic scale length of the zonal flow in nonlinear saturated stage. By treating the radial wavelength of the zonal flow as a parameter, the renormalization of the higher-order nonlinear effects was performed. The driving force of the zonal flow was derived, in which contributions of zonal flow vorticity at all orders were included. By use of this renormalized dynamical equation for the zonal flow, we studied the steady state system with both the drift wave fluctuations and zonal flows. The energy partition between them, the thermal conductivity, and the condition for the onset of drift wave turbulence were analyzed. The partition between the drift wave energy and zonal flow energy was obtained as a function of the growth rate of drift wave and the collisional damping of the zonal flow. A theoretical formula of the turbulent transport coefficient is derived, which covers the weakly unstable regime (no zonal flow), the moderately unstable regime (where the collisional damping of the zonal flow dictates the transport coefficient), and the strongly unstable case. The obtained formula extends the previously derived formula to wider circumstances. The condition for the onset of turbulence and turbulent transport in the collisionless limit was also derived. This explains what has been empirically known as Dimits shift in DNS. Formula of the turbulent transport coefficient was also derived, in which the screening effect by zonal flows is self-consistently included. The theoretical result was compared with the DNS. The energy partition between drift wave and zonal flow is tested for the relation $\chi_i(U)$. For a wide range of plasma parameters that control the growth rate of ITG mode instability, good agreement is also observed. Thus, this analysis captures some essential elements in the physics of the DW-ZF system. This theory also gives a prototypical example to understanding the mutual interaction between the turbulent energy transport and generation of axial vector field owing to the global gradient of plasma pressure.

Although this theory has shown some success in understanding of the nonlinear dynamics of DW-ZF system, further research is necessary. One issue is the parameter range of validity for the existence of the coherent structure of the zonal flow. The coherent time is finite in reality, and must be self-consistently determined by use of the statistical theory.^{3,24–27,43} Systematic continuation of this model and the BGK solution still needs further study. The decorrelation of drift wave at the low level of drift wave turbulence, Eq. (41), remains a very crude estimate in this article, and improve-

ment is necessary. The other issue is the application of methodology to various turbulence problems in actual experimental conditions. In both issues, future evolution of understanding is expected.

ACKNOWLEDGMENTS

Authors acknowledge discussions with Dr. M. Yagi, Dr. T. S. Hahm, Professor A. Fukuyama, and Professor H. Sanuki. This article is dedicated to Prof. Shoichi Yoshikawa on the occasion of his 70th birthday.

This work is partly supported by the Grant-in-Aid for Specially-Promoted Research of MEXT (16002005), by the Grant-in-Aid for Scientific Research of MEXT (15360495) and by the collaboration programs of NIFS and of the Research Institute for Applied Mechanics of Kyushu University, and by Asada Science Foundation. K.H. and P.H.D. acknowledge the hospitality of Kyushu University.

APPENDIX: A FORMULA OF TRANSPORT COEFFICIENT

In this appendix, explicit forms of the transport coefficient and the Dimits shift are discussed for a practical use.

An analytic estimate for D_{rr} has been given

$$D_{rr} \approx \frac{1}{B^2} \frac{k_\theta^2}{\gamma_L} |\tilde{\phi}|^2 \quad (\text{A1})$$

in the vicinity of the marginal condition $\Delta\omega_k \approx \gamma_L$ (See, e.g., Sec. 3.2.2 of Ref. 6). It is given, in terms of the normalized fluctuation amplitude, as $D_{rr} \approx (k_\theta^2 k_\perp^{-4}) \omega_*^2 \gamma_L^{-1} \hat{\phi}^2$. The growth rate of the zonal flow energy has been introduced by the definition $2D_{rr} q_r^2 = \alpha \hat{\phi}^2$. That is, the time rate α is given as

$$\alpha \approx \frac{\omega_*}{\gamma_L} \frac{2 k_\theta^2 q_r^2}{k_\perp^4} \omega_*. \quad (\text{A2})$$

The Dimits shift is given by the critical condition that satisfies Eq. (102), i.e.,

$$\gamma_{L,c} = \frac{4(1-\mu)^2 q_r^2}{\mu^2 H^2 k_\theta^2} \alpha. \quad (\text{A3})$$

Eliminating α from Eqs. (A2) and (A3), at $\gamma_L = \gamma_{L,c}$, one has an equation of the critical growth rate $\gamma_{L,c}$ as

$$\gamma_{L,c} = \frac{2\sqrt{2}(1-\mu) q_r^2}{\mu H k_\perp^2} \omega_*. \quad (\text{A4})$$

For the least stable mode, q_r is estimated by Eq. (57),

$$q_r \approx \frac{\sqrt{1-\mu}}{2} K_0,$$

this relation gives an estimate of $\gamma_{L,c}$,

$$\gamma_{L,c} = \frac{(1-\mu)^2 K_0^2}{\sqrt{2\mu} H k_\perp^2} \omega_*. \quad (\text{A5})$$

One estimate for $K_0 = k_r$:

$$\gamma_{L,c} = \frac{(1-\mu)^2 k_r^2}{\sqrt{2\mu} H k_\perp^2} \omega_*. \quad (\text{A6})$$

For parameters $\mu \approx 1/2$, $\gamma_{L,c}$ is of the order of one-tenth of ω_* .

Explicit forms are also derived for domains discussed in Sec. IV B 2. One has the following expressions.

(a) Small growth rate limit:

In the case of weak instability, i.e.,

$$\gamma_L < \frac{1}{(1-\mu)} \frac{k_\perp^4}{k_\theta^2 q_r^2} \nu_{\text{damp}} \quad (\text{region I}), \quad (\text{A7})$$

the fluctuation level is given by

$$\hat{\phi} = \frac{\gamma_L}{\omega_*} \equiv \hat{\phi}_I. \quad (\text{A8})$$

(b) Intermediate growth rate limit:

For the case of

$$\frac{1}{(1-\mu)} \frac{k_\perp^4}{k_\theta^2 q_r^2} \nu_{\text{damp}} < \gamma_L < \gamma_{L,c} \quad (\text{region II}) \quad (\text{A9})$$

the fluctuation level is given by

$$\hat{\phi} = \frac{1}{\sqrt{1-\mu}} \frac{k_\perp^2}{k_\theta q_r} \sqrt{\frac{\nu_{\text{damp}} \gamma_L}{\omega_* \omega_*}} \equiv \hat{\phi}_{II}. \quad (\text{A10})$$

(c) Large growth rate limit

The transition from the collisional-damping-dominated region [region II] to the nonlinearity-dominated region is expected to occur at

$$\frac{1}{\mu H \rho_s^2 k_\theta^2} \nu_{\text{damp}} + \gamma_{L,c} < \gamma_L \quad (\text{region III}). \quad (\text{A11})$$

One has, from Eq. (87),

$$\begin{aligned} \frac{\Delta\omega_k}{\omega_*} \approx & \frac{\mu H \rho_s^2 k_\perp^4}{4(1-\mu) q_r^2} \left(-1 \right. \\ & \left. + \sqrt{1 + \frac{8(1-\mu) q_r^2}{\mu H \rho_s^2 k_\perp^4} \left(\frac{\gamma_L - \gamma_{L,c}}{\gamma_L} \right)} \right) \\ & \times \frac{\gamma_L}{\omega_*} \equiv \hat{\phi}_{III}. \end{aligned} \quad (\text{A12})$$

The asymptotically-linear dependence on γ_L in this model is recovered, and a suppression factor appears. The suppression factor, which is induced by the co-existence of the zonal flow, is approximately evaluated as $\sqrt{\mu H / 2(1-\mu) \rho_s k_\perp^2 q_r^{-1}} \sim k_\perp \rho_s$.

A similar argument is possible for the thermal conductivity. In regions I and II, a fitting formula is given as

$$\chi_{I+II} = \frac{\gamma_L \sqrt{\nu}}{\sqrt{\gamma_L + \sqrt{\nu}} k_r}, \quad (\text{A13})$$

where

$$\nu = \frac{1}{(1-\mu)} \frac{k_{\perp}^4}{k_{\theta}^2 q_r^2} \nu_{\text{damp}} \quad (\text{A14})$$

denotes the impact of collisional damping of the zonal flow. In region III, Eq. (93) and Eq. (A12) provide

$$\chi_{\text{III}} = \frac{\mu H \rho_s^2 k_{\perp}^4}{4(1-\mu) q_r^2} \left(-1 + \sqrt{1 + \frac{8(1-\mu) q_r^2}{\mu H \rho_s^2 k_{\perp}^4} \left(\frac{\gamma_L - \gamma_{L,c}}{\gamma_L} \right)} \right) \frac{\gamma_L}{k_r^2}. \quad (\text{A15})$$

A fitting in regions I, II, and III is

$$\chi_i = \chi_{\text{fit}} \equiv \sqrt{\chi_{\text{I+II}}^2 + \chi_{\text{III}}^2 \Theta(\gamma_L - \gamma_{L,c})}, \quad (\text{A16})$$

where $\Theta(\gamma_L - \gamma_{L,c})$ is a Heaviside function.

¹A. Yoshizawa, S.-I. Itoh, and K. Itoh, *Plasma and Fluid Turbulence* (IOP, Bristol, 2002)

²C W Horton, *Rev. Mod. Phys.* **71**, 735 (1999).

³P. H. Diamond, M. N. Rosenbluth, F. L. Hinton, M. Malkov, J. Fleisher, and A. Smolyakov, *17th IAEA Fusion Energy Conference, Yokohama, 1998*, International Atomic Energy Agency, Vienna, 1998, paper IAEA-CN-69/TH3/1; P. H. Diamond, S. Champeaux, M. Malkov *et al.*, *Nucl. Fusion* **41**, 1067 (2001).

⁴A. Hasegawa and M. Wakatani, *Phys. Rev. Lett.* **59**, 1581 (1987).

⁵G. W. Hammett, M. A. Beer, W. Dorland, S. C. Cowley, and S. A. Smith, *Plasma Phys. Controlled Fusion* **35**, 973 (1993).

⁶P. H. Diamond, K. Itoh, S.-I. Itoh, and T. S. Hahm, *Plasma Phys. Controlled Fusion* **47**, R35 (2005).

⁷A. Fujisawa, K. Itoh, H. Iguchi, K. Matsuoka, S. Okamura, A. Shimizu, T. Minami, Y. Yoshimura, K. Nagaoka, C. Takahashi, M. Kojima, H. Nakano, S. Ohsima, S. Nishimura, M. Isobe, C. Suzuki, T. Akiyama, K. Ida, K. Toi, S.-I. Itoh, and P. H. Diamond, *Phys. Rev. Lett.* **93**, 165002 (2004).

⁸A. Yoshizawa, S.-I. Itoh, K. Itoh, and N. Yokoi, *Plasma Phys. Controlled Fusion* **46**, R25 (2004).

⁹For a review, see for example, P. H. Diamond, D. W. Hughes, and E.-J. Kim, in *The Fluid Mechanics of Astrophysics and Geophysics* edited by A. M. Soward, C. A. Jones, D. W. Hughes, and N. O. Weiss (Taylor & Francis, CRC, London, 2005), Vol. 12, p. 145.

¹⁰Z. Lin, T. S. Hahm, W. W. Lee, W. M. Tang, and P. H. Diamond, *Phys. Rev. Lett.* **83**, 3645 (1999).

¹¹A. M. Dimits, G. Bateman, M. A. Beer *et al.*, *Phys. Plasmas* **7**, 969 (2000).

¹²H. Sugama, T. H. Watanabe, and W. Horton, *Phys. Plasmas* **10**, 726 (2003).

¹³K. Hallatschek, *Phys. Rev. Lett.* **93**, 065001 (2004).

¹⁴B. N. Rogers, W. Dorland, and M. Kotschenreuther, *Phys. Rev. Lett.* **85**,

5336 (2000).

¹⁵F. Jenko, B. Scott, W. Dorlandy, A. Kendl, and D. Strintzi, presented at *19th IAEA Conference on Fusion Energy, Lyon, 2002*, International Atomic Energy Agency, Vienna, 2002, paper TH/1-2.

¹⁶Y. Idomura, M. Wakatani, and S. Tokuda, *Phys. Plasmas* **7**, 3551 (2000).

¹⁷J. Li, Y. Kishimoto, Y. Idomura, N. Miyato, T. Matsumoto: *J. Plasma Fusion Res.* **6**, 581 (2005).

¹⁸E.-J. Kim and P. H. Diamond, *Phys. Plasmas* **9**, 4530 (2002).

¹⁹K. Hallatschek, *Phys. Rev. Lett.* **84**, 5145 (2000).

²⁰A. Smolyakov and P. H. Diamond, *Phys. Rev. Lett.* **84**, 491 (2000).

²¹Liu Chen, Z. Lin, and R. White, *Phys. Plasmas* **7**, 3129 (2000).

²²P. Kaw, R. Singh, and P. H. Diamond, *Plasma Phys. Controlled Fusion* **44**, 51 (2002).

²³V. S. Marchenko, *Phys. Rev. Lett.* **89**, 185002 (2002).

²⁴R. Balescu, *Phys. Rev. E* **68**, 046409 (2003).

²⁵S.-I. Itoh and K. Itoh, *J. Phys. Soc. Jpn.* **69**, 408 (2000); **69**, 3253 (2000).

²⁶S.-I. Itoh and K. Itoh, *J. Phys. Soc. Jpn.* **69**, 427 (2000).

²⁷J. A. Krommes and C. B. Kim, *Phys. Rev. E* **62**, 8508 (2000).

²⁸M. A. Malkov and P. H. Diamond, *Phys. Plasmas* **8**, 3996 (2001).

²⁹M. A. Malkov, P. H. Diamond, and M. N. Rosenbluth, *Phys. Plasmas* **8**, 5073 (2001).

³⁰K. Itoh and S. I. Itoh, *Plasma Phys. Controlled Fusion* **38**, 1 (1996).

³¹K. Itoh, S.-I. Itoh, and A. Fukuyama, *Transport and Structural Formation in Plasmas* (IOP, Bristol, England, 1999).

³²K. Itoh, K. Hallatschek, S. Toda, H. Sanuki, and S.-I. Itoh, *J. Phys. Soc. Jpn.* **79**, 2921 (2004).

³³K. Itoh, K. Hallatschek, S. Toda, S.-I. Itoh, P. H. Diamond, M. Yagi, and H. Sanuki, *Plasma Phys. Controlled Fusion* **46**, A335 (2004).

³⁴T. S. Hahm, K. H. Burrell, Z. Lin, R. Nazikian, and E. J. Synakowski, *Plasma Phys. Controlled Fusion* **42**, A205 (2000).

³⁵K. Hallatschek and P. H. Diamond, *New J. Phys.* **5**, 29.1 (2003).

³⁶M. N. Rosenbluth and F. L. Hinton, *Phys. Rev. Lett.* **80** 724 (1998).

³⁷A. Yoshizawa, *Hydrodynamics and Magnetohydrodynamic Turbulent Flows* (Kluwer, Dordrecht, 1998).

³⁸P. H. Diamond, K. Itoh, S.-I. Itoh, and T. S. Hahm, "Granulation formation and turbulent trapping in wave kinetics" (2004) presented at Fields Institute.

³⁹P. H. Diamond, Y.-M. Liang, B. A. Carreras, and P. W. Terry, *Phys. Rev. Lett.* **72**, 2565 (1994).

⁴⁰R. E. Waltz, G. M. Staebler, W. Dorland, G. Hammett, M. Kotschenreuther, and J. A. Konings, *Phys. Plasmas* **4**, 2482 (1997).

⁴¹P. H. Diamond, K. Itoh, S.-I. Itoh, and T.-S. Hahm, "Overview of zonal flow physics," presented at *the 20th IAEA Fusion Energy Conference, Vilamoura, Portugal, 2004*, International Atomic Energy Agency, Vienna, 2004, paper OV/2-1.

⁴²Z. Lin and T. S. Hahm, *Phys. Plasmas* **11**, 1099 (2004).

⁴³S.-I. Itoh, K. Itoh, and S. Toda, *Phys. Rev. Lett.* **89**, 215001 (2002); *Plasma Phys. Controlled Fusion* **45**, 823 (2003); S.-I. Itoh, K. Itoh, M. Yagi, and S. Toda, *ibid.* **46**, A341 (2004).